A SPIKE1 signaling complex controls actin-dependent cell morphogenesis through the heteromeric WAVE and ARP2/3 complexes

Dipanwita Basu*, Jie Le†, Taya Zakharova, Eileen L. Mallery, and Daniel B. Szymanski‡

Department of Agronomy, Purdue University, Lilly Hall, 915 W. State Street, West Lafayette, IN 47907-2054

Edited by Brian A. Larkins, University of Arizona, Tucson, AZ, and approved January 10, 2008 (received for review October 30, 2007)

During morphogenesis, the actin cytoskeleton mediates cell-shape change in response to growth signals. In plants, actin filaments organize the cytoplasm in regions of polarized growth, and the filamentous arrays can be highly dynamic. Small GTPase signaling proteins termed Rho of plants (ROP)/RAC control actin polymerization. ROPs cycle between inactive GDP-bound and active GTP-bound forms, and it is the active form that interacts with effector proteins to mediate cytoskeletal rearrangement and cell-shape change. A class of proteins termed guanine nucleotide exchange factors (GEFs) generate GTP–ROP and positively regulate ROP signaling. However, in almost all experimental systems, it has proven difficult to unravel the complex signaling pathways from GEFs to the proteins that nucleate actin filaments. In this article, we show that the DOCK family protein SPIKE1 (SPK1) is a GEF, and that one function of SPK1 is to control actin polymerization via two heteromeric complexes termed WAVE and actin-related protein (ARP) 2/3. The genetic pathway was constructed by using a combination of highly informative *spk1* alleles and detailed analyses of *spk1*, *wave*, and *arp2/3* single and double mutants. Remarkably, we find that in addition to providing GEF activity, SPK1 associates with WAVE complex proteins and may spatially organize signaling. Our results describe a unique regulatory scheme for ARP2/3 regulation in cells, one that can be tested for widespread use in other multicellular organisms.

DOCK | cytoskeleton | guanine nucleotide exchange factor | Rho GTPase | ROP

Cell morphogenesis occurs in the context of tissue and organ development. In the leaf epidermis, populations of cells regulate the location and extent of cell expansion, primarily through the spatial control of the cytoskeleton and endomembrane systems. Plant cells (1, 2), like those of other eukaryotes (3, 4), use Rho family small GTPases as critical signaling proteins to dictate cell-shape change. Rho of plants (ROP) cycles between GTP-bound active forms and GDP-bound inactive forms, and the nucleotide status of ROP is subject to complex regulation. One class of proteins termed guanine nucleotide exchange factors (GEFs) catalyzes the exchange of bound GDP with the endogenous pool of GTP and positively regulates ROP signaling (2, 4). GTP-bound ROP physically interacts with diverse classes of effector proteins to control trafficking through the endomembrane system and the organization of the cytoskeleton (5–7). This article defines a complete morphogenetic pathway from ROP activation to actin-related protein (ARP) 2/3-dependent regulation of the actin cytoskeleton.

In the leaf epidermis, three different ROP effectors are known. *Interactor of constitutive active ROPs 1* (*ICR1*) is required for the polarized growth and the normal lobing of pavement cells and appears to link ROP signaling to the exocyst complex and the secretory pathway (7). Two other genes, *Rop-interactive CRIB motif 4* (*RIC4*) (6) and *PIROGI/KLUNKER/PIRP/SRA1* (referred to in this article as *SRA1*) (5), are thought to link ROP signaling to actin-dependent polarized growth. The genetic and biochemical functions of SRA1 are well characterized. SRA1 is a conserved protein in both plants and animals and is a WAVE complex protein that directly interacts with active ROP/Rac (5, 8). In cultured mammalian cells, Sra1 mediates the Rac-dependent relocalization of the WAVE complex to leading edges of lamellipodia (9), and in *Arabidopsis*, SRA1 and the WAVE complex positively regulate an actin filament-nucleating machine, named the ARP2/3 complex (10). Plant and animal WAVE complexes contain SCAR, a potent activator of ARP2/3-dependent actin filament nucleation (8, 11).

In both plant and animal systems, the proteins that generate the ROP/Rac signals and activate the WAVE–ARP2/3 pathway are not known, and in general it has proven difficult to assign clear functional linkages between GEFs and the proteins that directly regulate the cytoskeleton. To our knowledge, a genetic pathway linking a specific GEF to an actin filament nucleator has not been described in any multicellular organism. Progress is hindered by genetic redundancy. For example, vertebrate genomes encode large gene families of Dbl-homology domain and DOCK family RhoGEFs (3, 4). In other cases, genetic studies of nonredundant GEFs (12) or actin filament nucleators (13) are complicated by extreme pleiotropy and/or embryonic lethality. Genetic studies in *Arabidopsis* are not immune to such technical barriers. Although plants appear to lack the Dbl-homology domain-containing RhoGEFs that are widespread in animals, the *Arabidopsis* genome encodes 14 PRONE domain GEFs (14) that can affect the actin cytoskeleton and the tip growth of pollen tubes (15, 16). *Arabidopsis* has only a single DOCK family protein, SPIKE1 (SPK1). *SPK1* (17), like all known *WAVE* and *ARP2/3* complex subunit genes (11), is ubiquitously expressed and, based on the presence of the conserved DOCK homology region 2 (DHR2) domain, SPK1 originally was proposed to positively regulate ROP (17). Although the phenotype of *spk1* plants is quite pleiotropic, the viability of the mutant and its highly diagnostic trichome-swelling phenotype can be used to discover novel morphogenesis pathways.

In this article, we exploit a set of *Arabidopsis* epidermal morphology mutants termed the "distorted group" to define a morphogenesis pathway from the DOCK family GEF SPK1 to the actin filament nucleator ARP2/3. Our genetic and biochemical data indicate that ROP activation is the critical function for SPK1. We find that SPK1 not only generates signals that activate

Author contributions: D.B. and J.L. designed research; D.B., J.L., and T.Z. performed research; E.L.M. contributed new reagents/analytic tools; and D.B.S. wrote the paper.

The authors declare no conflict of interest.

This article is a PNAS Direct Submission.

*Present address: Department of Microbiology, University of Virginia School of Medicine, Charlottesville, VA 22908.

†Present address: Department of Botany, University of British Columbia, Vancouver, BC, Canada V6T 1Z4.

‡To whom correspondence should be addressed. E-mail: dszyman@purdue.edu.

This article contains supporting information online at www.pnas.org/cgi/content/full/0710294105/DC1.

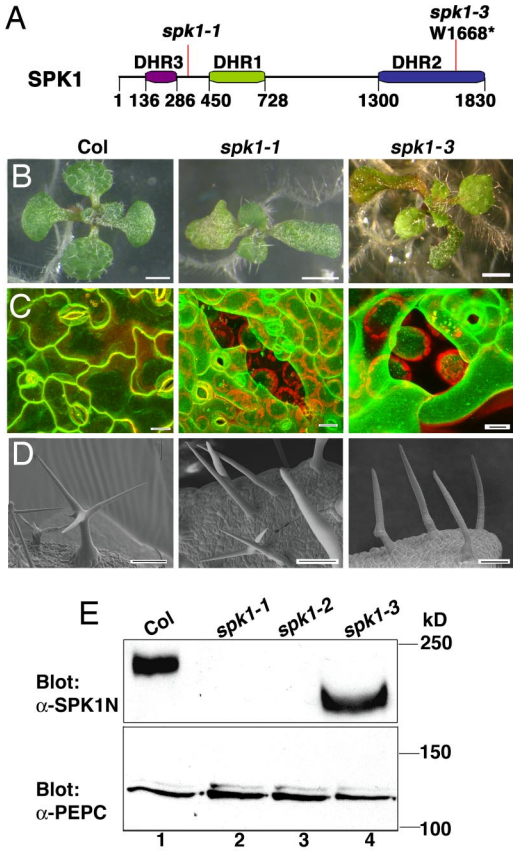

Fig. 1. The SPK1 Dock homology region 2 (DHR2) domain provides critical functions *in vivo*. (*A*) The domain organization of SPK1 protein. The locations of the *spk1-1* and *spk1-3* mutations are indicated. The conserved regions of SPK1 are labeled. (*B*) Wild-type, *spk1-1*, and *spk1-3* seedlings at 10 DAG. (*C*) Pavement cell–cell adhesion defects of *spk1* cotyledons and leaves. Wild-type, *spk1-1*, and *spk1-3* seedlings were stained with 0.1 μM FM1–43 (green) to visualize cell boundaries. The autofluorescence from the chloroplasts of the underlying mesophyll cells is red and is clearly visible within pavement cell gaps. (*D*) SEM of stage 6 mature trichomes from wild-type, *spk1-1*, and *spk1-3* leaves, respectively. (*E*) The truncated *spk1*-3 accumulates. (*Upper*) Lanes 1–4, Western blot analysis of protein of whole-cell extracts of wild-type, *spk1-1*, *spk1-2*, and *spk1-3* plants, respectively, probed with α-SPK1N antibody. (*Lower*) Western blot analysis with same extracts as in *Upper* but probed with a α-PEPC antibody for a loading control. [Scale bars: 1 cm (*B*), 10 μm (*C*), and 100 μm (*D*).]

the WAVE–ARP2/3 pathway, but also that the ROP–GEF associates with downstream WAVE complex targets of ROP signaling.

Results

The DOCK family protein SPK1 contains a C-terminal segment that shares amino acid identity with the catalytic domain of DOCK family GEFs (17–19). To test for an *in vivo* importance of SPK1 and its putative GEF domain, termed DHR2 (18) or CDMS (17), we analyzed a *spk1-3* allele that truncated ≈160 aa from the domain (Fig. 1*A*). The mutation caused *spk1* null phenotypes (Fig. 1 *B–D*). Compared with the wild-type trichomes, those of *spk-1* and *spk1-3* showed a reduced branch number and an irregular swelling along the stalk and branches (Fig. 1*D*). The null *spk1-3* phenotype was not caused by destabilization of the truncated protein, because in whole-cell extracts, *spk1-3* accumulated to approximately wild-type levels (Fig. 1*E*). Given the highly conserved amino acid sequence and known function of DH2 domains, the above results suggest that positive regulation of ROP is a critical function for SPK1.

We therefore tested the ability of endogenous SPK1 to associate with ROP. In coimmunoprecipitation (coIP) experiments using an antibody directed against SPK1, we found that endogenous SPK1 and ROP associated with each other (Fig. 2*A*). DHR2 affected the formation of SPK1–ROP complexes because we failed to detect ROP in coIP experiments using extracts prepared from *spk1-3* plants (Fig. 2*A*). DHR2 also mediated the association of SPK1 with ROP in pull-down assays using purified GST-tagged ROPs. The preferential binding to a nucleotide-depleted Rho apoprotein is a hallmark of GEFs (4), and we found that endogenous SPK1 associated with GST–ROP2 in either the nucleotide-depleted or the GDP-bound forms (Fig. 2*B*). As expected, the association required an intact DHR2 domain (Fig. 2*B*). Furthermore, the interaction was specific to ROP, because SPK1 binding to human Rac was not detected (Fig. 2*B*). SPK1 and ROP directly interact because a purified C-terminal fragment of SPK1 (996-DHR2) efficiently sedimented inactive forms of ROP2 (Fig. 2*C*). We suspect that the previously reported failure to detect direct interactions between SPK1 and ROP (14) reflects a weakness of the yeast two-hybrid assay.

The *Arabidopsis* ROP GTPase gene family consists of 11 members (20), many of which are expressed in the shoot and are candidate targets of SPK1 regulation. We therefore tested the SPK1-binding activity of several shoot-expressed prenylated ROPs (ROP2 to ROP5) and the S-acylated isoform, ROP10 (21). In triplicate pull-down assays that used full-length recombinant SPK1, there were no significant differences in the strength of SPK1 binding to any of the different ROP isoforms (Fig. 2*D*). However, for each of the ROPs tested, SPK1-binding was highly selective for nucleotide-depleted or GDP-bound forms [Fig. 2*D* and supporting information (SI) Fig. 5]. The ability of SPK1 and 996-DHR2 to bind GDP–ROP is unique compared with other known DOCKs, such as Dock180 and Zizimin (18, 19, 22). Full-length recombinant SPK1 has GEF activity. The intrinsic rate of ROP2 nucleotide exchange was slow with an apparent off-rate of bound nucleotide (k_{obs}) of 0.03 min^{-1}, and SPK1 accelerated the nucleotide exchange reaction ≈7-fold (Fig. 2*E*), with k_{obs} = 0.21 min^{-1}. Insect extracts containing an irrelevant expressed protein had no effect on the reaction kinetics (Fig. 2*E*). The DHR2 domain is sufficient for GEF activity because purified 996-DHR2 accelerated nucleotide exchange ≈4-fold (k_{obs} = 0.13 min^{-1}), and the activity increased in a concentration-dependent manner (Fig. 2*F*). The nucleotide exchange activity of 996-DHR2 is at least as strong as those reported for DHR2 fragments from Dock180 and Zizimin1 (18, 19). SPK1 catalysis was not limited to ROP2 as a substrate. The full-length protein accelerated nucleotide exchange when tested with ROP3, ROP4, and ROP6 (SI Fig. 6). Together, these biochemical data suggest that endogenous SPK1 is sufficient to bind and activate endogenous ROP.

The trichome phenotypes of *spk1* provide an opportunity to identify additional genes that couple SPK1 GEF activity to a cytoskeletal response. *Spk1*$^{-}$ trichomes often are swollen and short (Figs. 1*D* and 3 *A* and *F*). These phenotypes resemble those of the "distorted group," which is a set of mutants that corresponds to *WAVE* and *ARP2/3* subunit-encoding genes (10). Like the distorted mutants (23, 24), the reduced length and irregular swelling of *spk1* are relatively insensitive to actin-depolymerizing drugs such as latrunculin B (LatB) (Fig. 3*E*). A reduced trichome branch number does not preclude LatB-induced swelling, because the drug clearly enhanced the cell swelling of *gl3* and qualitatively phenocopied *spk1* trichomes (Fig. 3*C*). The cytoskeleton defects in swollen *spk1* branches also are consistent with an ARP2/3-related component to the phenotype. Unlike early-stage wild-type branches that contained a population of cytoplasmic actin filaments and bundles that extended toward the branch apex, similarly staged swollen *spk1* branches failed to

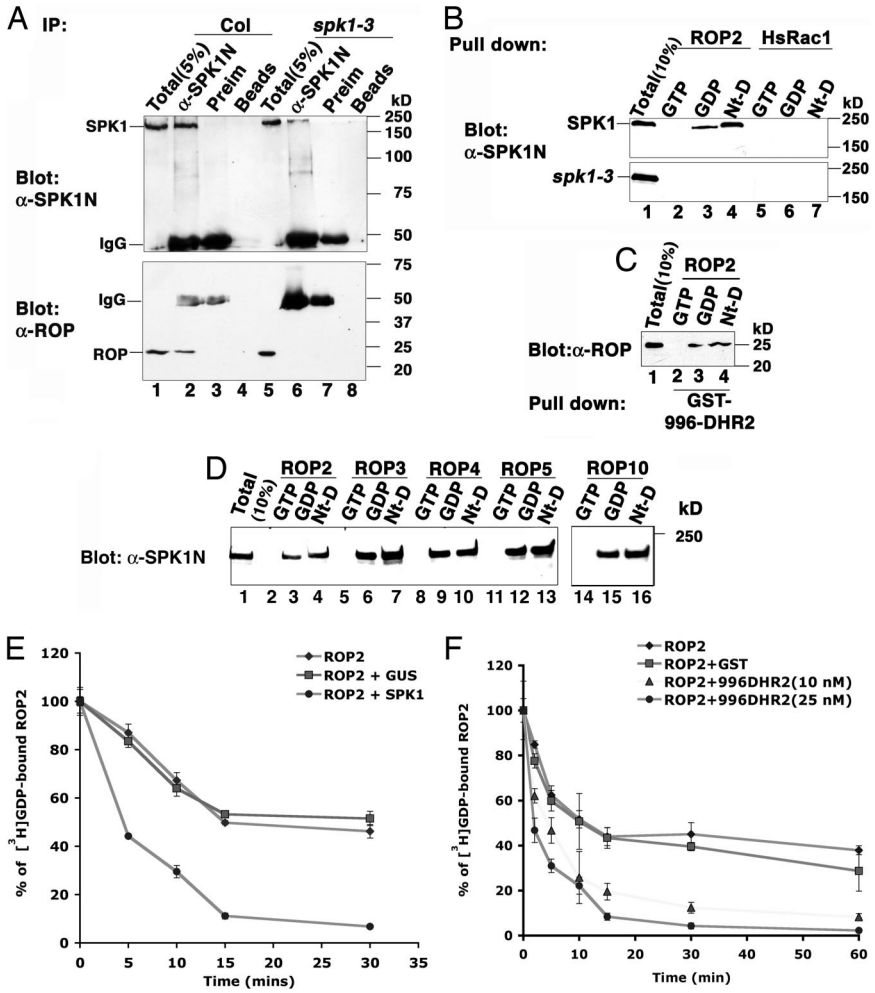

Fig. 2. SPK1 binds to ROPs in a DHR2-dependent manner and facilitates nucleotide exchange. (*A*) Endogenous SPK1–ROP complexes require an intact DHR2 domain. Lanes 1 and 5, 5% of input solubilized protein extracts; lanes 2–4, proteins immunoprecipitated from wild-type extracts using α-SPK1N antibody, preimmune serum, and protein A beads alone, respectively; lanes 6–8, same conditions as above but with *spk1-3* extracts. coIP fractions were probed with α-SPK1N (*Upper*) and α-ROP (*Lower*) antibodies. (*B*) Endogenous SPK1 associates specifically with inactive forms of ROP2 in a DHR2-dependent manner. GTP-bound, GDP-bound, or nucleotide-depleted (Nt-D) GST–ROP2 and human GST–Rac1 were bound to beads and incubated with cytosolic fractions from wild-type (*Upper*) and *spk1-3* (*Lower*) plants. Bound fractions were probed with α-SPK1N antibodies. (*C*) Recombinant purified 996-DHR2 interacts directly with ROP in a nucleotide-dependent manner. Lane 1, 10% of the input fraction; lanes 2–4, the GST-996-DHR2 bound fractions of GTP-loaded, GDP-loaded, or Nt-D HIS–ROP2, respectively. Bound fractions were probed with an α-ROP antibody. (*D*) Recombinant full-length SPK1 interacts directly with inactive ROPs. GTP-bound, GDP-bound, or Nt-D GST–ROPs were used in GST pull-down assays with recombinant full-length SPK1 expressed in insect SF9 cells. Lane 1, 10% of total input SPK1; lanes 2–25, Western blots of bound, pellet fractions probed with the α-SPK1N antibody. (*E*) Full-length SPK1 has guanine nucleotide exchange activity *in vitro*. Purified ROP2 was loaded with [^{3}H]GDP, and exchange reactions were initiated by the addition of 100-fold molar excess of unlabeled GTP and SPK1. Controls included no additional proteins and SF9 extracts containing an irrelevant protein. Each time point is shown as the mean ± SD of triplicate measurements. (*F*) The 996-DHR2 fragment of SPK1 has GEF activity. GEF assays were performed as described above except the reactions include varying amounts of 996-DHR2.

generate or maintain such an array (Fig. 3*B*). As reported (5, 25), *sra1* trichome branches also have disorganized core actin filaments (Fig. 3*B*). *Spk*$^-$ shared several additional phenotypes with *wave* and *arp2/3* mutants, including defective pavement cell–cell adhesion (Fig. 1*C*) and a reduced length and cell–cell adhesion in etiolated hypocotyls (SI Fig. 7 and SI Table 1), further suggesting that these genes function in a common pathway.

To test directly for *SPK1* and *SRA1* functions in a common pathway, we constructed double mutants and used trichome height and a shape descriptor for cell swelling to quantitate cell-shape phenotypes. If *SPK1* and *SRA1* function in independent growth pathways, then we would expect the double mutant to display a phenotype that is more severe than *spk1* alone. However, the cell height and swelling phenotypes of *spk1 sra1* were indistinguishable from those of *spk1* alone (Fig. 3 *E* and *F*), indicating that the genes function in a common pathway. Our trichome shape assays resolved genes that function in *SRA1*-independent pathways because *gl3 sra1* (Fig. 3 *C* and *D*) and *sti sra1* (SI Fig. 8 and SI Table 2) trichomes were significantly shorter and more swollen compared with *gl3* and *sti* alone. The double mutants also revealed independent trichome functions for both *SPK1* and *SRA1*. As expected, in *spk1 sra1*, the reduced branch number phenotype of *spk1* was independent of *SRA1* (Fig. 3 *A* and *E*). Along similar lines, distorted mutants have a cell-twisting component to their trichome phenotype. *Spk1*$^-$ trichomes do not twist (Fig. 1*D* and 3*A*), but as expected, the twisting phenotype of *sra1* was apparent in a double mutant combination with *spk1* (Fig. 3*E*) and *gl3* (Fig. 3*C*).

These genetic data indicate that *SPK1* and *SRA1* function in a common pathway that prevents cell swelling and suggest that *SPK1*-dependent activation of ROP is the primary mechanism of *SRA1* activation. However, the connectivity and specificity of the

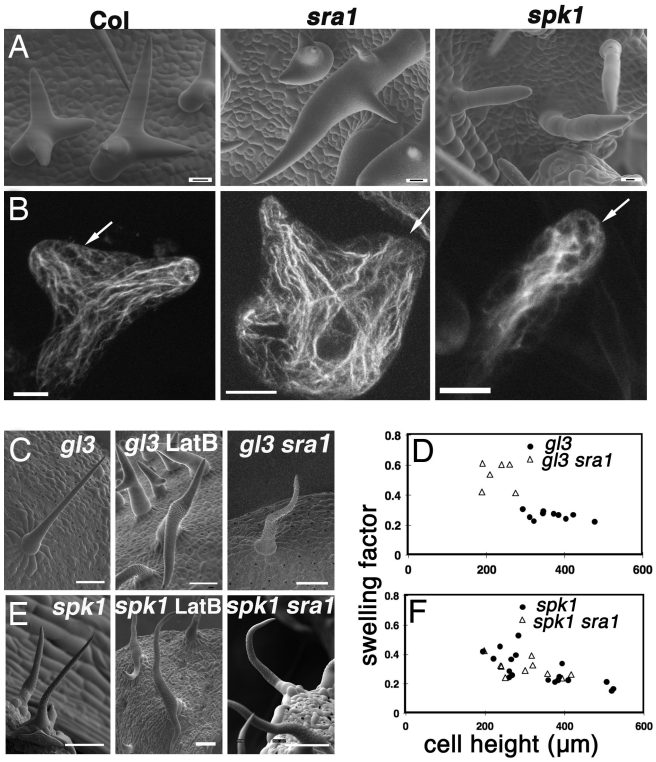

Fig. 3. *SPK1* and the WAVE complex gene *SRA1* function in a common pathway that controls polarized growth. (*A*) *sra1* and *spk1* trichomes have a cell-swelling component to their phenotype. SEM of young wild-type (Col), *sra1*, and *spk1* trichomes. (Scale bar: 20 μm.) (*B*) Actin filament networks are disorganized in the core cytoplasm of growing *spk1* and *sra1* trichomes. Actin filaments in whole mounted Col, *sra1*, and *spk1* trichomes were visualized with Alexa 488-phalloidin as described in ref. 5. Confocal images are maximum projections of the entire cell. Arrows indicate developing branch regions that normally contain aligned core actin bundles. (Scale bar: 10 μm.) (*C* and *D*) *sra1* enhances the cell swelling of the reduced branching mutant *glabra3*. (*C*) SEM of the mature trichomes: *gl3*, *gl3* treated with Lat B, and *gl3 sra1*. (*D*) Quantitative analysis of single and double mutant trichome phenotypes. Cell length was plotted against swelling factor. Swelling factor is measured from orthogonal views and is a dimensionless value based on the perimeter/area ratio of an equilateral triangle (see *Materials and Methods*). (*E* and *F*) *spk1* and *spk1 sra1* trichomes have indistinguishable swelling phenotypes. (*E*) SEM of the mature trichomes: *spk1*, *spk1* treated with Lat B, and *spk1 sra1*. (*F*) Quantitation of the cell swelling and cell length phenotypes of *spk1* and *spk1 sra1* as described in *D*. (Scale bar: 50 μm.)

SPK1–ROP–SRA1 pathway is not clear, because SPK1 appears to bind and activate ROPs promiscuously. Importantly, SRA1 may associate with active ROPs with a greater degree of isoform specificity (5). In GST pull-down assays, SRA1 consistently bound most strongly to GTP–ROP2 and GTP–ROP4 (Fig. 4*A*). SRA1 had weaker physical interactions with GTP–ROP3 and GTP–ROP6, and no binding to ROP5 and ROP10 was detected even though they were active proteins, because both ROPs associated with MBP–RIC1 with nucleotide selectivity (Fig. 4*A*).

To learn more about the coupling of SPK1, ROP, and WAVE activities, we tested for physical associations between SPK1 and WAVE complex proteins. GEFs have been reported to physically interact with putative effector proteins (26), and it is possible that SPK1 could increase signaling specificity by associating with components of the WAVE complex. Our SRA1 antibodies did not detect the endogenous protein in Western blots. However, NAP1 is a useful surrogate for SRA1 because the plant proteins physically interact with high affinity (27), and in vertebrate cells Sra1 and Nap1 copurify (8). Immunoprecipitates of solubilized endogenous SPK1 contained the WAVE complex protein NAP1 (Fig. 4*B*). The association of SPK1 and NAP1 is specific because NAP1 was not detected in preimmune serum coIP fractions, and only background signals were obtained when *spk1-1* extracts were used as the source of proteins (Fig. 4*B*). These data indicate that at least some fraction of endogenous SPK1 and NAP1 exist as a complex. As an independent test for an association of SPK1 with WAVE complex proteins, we analyzed the size of detergent-solubilized SPK1 complexes isolated from wild-type, *sra1*, and *nap1* strains (Fig. 4*C*). If a significant pool of SPK1 associates with SRA1 (145 kDa) and/or NAP1 (149 kDa), then we would expect SPK1 complexes to shift to lower mass fractions in the mutant backgrounds. In wild-type extracts, SPK1 complexes had a mean apparent mass of 660 kDa and were distributed normally across three gel-filtration fractions. Even after overexposure of Western blots, SPK1 signal was restricted to these three fractions. In the *sra1* background, the apparent mass of SPK1 complexes was clearly reduced, and SPK1 was consistently observed also in a 280-kDa fraction (Fig. 4*C*). Removal of NAP1 had a more subtle effect on SPK1. In *nap1*, the peak fraction for SPK1 was reproducibly shifted to a mean apparent mass of 530 kDa, and SPK1 signal in 340-kDa fractions was consistently detected (Fig. 4*C*). The more severe effects of *sra1*, compared with *nap1*, on the size distribution of SPK1 complexes may reflect a more prominent role for SRA1 in the recruitment or stabilization of SPK1 complex proteins, including its binding partner NAP1. The association of endogenous SPK1 with WAVE complex proteins is consistent with the hypothesis that SPK1 directly regulates the WAVE–ARP2/3 pathway and presents a possible mechanism to generate signaling specificity.

Discussion

In this article, we report on the discovery of a morphogenetic pathway in which the ROP–GEF SPK1 positively regulates actin-dependent morphogenesis through the heteromeric WAVE and ARP2/3 complexes. The pathway was constructed by using informative null alleles, clear genetic interactions, and biochemical activities of pathway components. The basic regulatory scheme is clear. SPK1 is a GEF that generates GTP–ROP. SRA1 is one target of SPK1 signaling, and through unknown mechanisms, SRA1 translates GTP–ROP signals into positive regulation of the ARP2/3 complex during actin-dependent growth. This pathway controls numerous aspects of plant development (25) and presents an important opportunity to understand how cellular activities are coordinated during growth.

Our genetic analyses strongly support the existence of a *SPK1–WAVE–ARP2/3* pathway. First, the similar array of *spk1*, *wave*, and *arp2/3* phenotypes suggests common functions. *Spk1*$^-$ trichomes, unlike those of other reduced branching mutants *sti* and *gl3*, are swollen and not noticeably affected by actin-depolymerizing drugs, and the actin cytoskeleton is disorganized in apical regions of elongating cells. In addition *spk1*, *wave*, and *arp2/3* mutants display reduced pavement cell–cell adhesion and indistinguishable hypocotyl elongation defects—all defining features of the distorted group mutants (10). Our double mutant analysis of *spk1 sra1* indicates clearly that *SPK1* and the ROP signaling target *SRA1* function in a common pathway, because the trichome swelling and cell elongation defects of *spk1* are indistinguishable from those of the double mutant.

Our results provide clear insight into the regulatory relationships between SPK1 and the WAVE complex. We find that the conserved DHR2 domain of SPK1 provides critical GEF activity. Truncation of the domain causes a *spk1* null phenotype and affects the ability of endogenous SPK1 to associate with ROP in both coIP and GST–ROP pull-down assays. We also find that the purified DHR2 domain is sufficient for ROP-binding and GEF activity. Significantly, we detect stable physical associations of

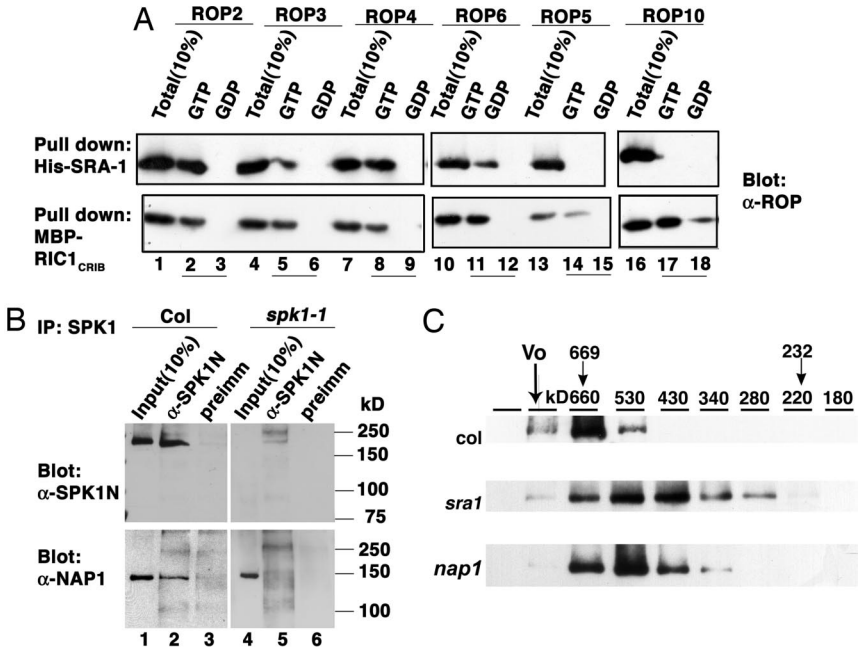

Fig. 4. The WAVE complex protein SRA1 is a ROP effector, and endogenous SPK1 and WAVE complex proteins form complexes. (*A*) SRA1 is an effector for a subset of ROPs. Soluble, purified GST–ROPs were pulled down with bead-bound HIS–SRA1 (*Upper*) and MBP–RIC1 (*Lower*) and probed with a α-ROP antibody. The input fraction and the bead-bound fractions from each ROP binding reaction are labeled. The nucleotide status of ROP in each reaction is indicated. (*B*) Endogenous SPK1 associates with the WAVE complex subunit NAP1 in cells. coIP of SPK1 was performed as described in Fig. 2*A*. (*Upper*) Lanes 1 and 4, 10% of input protein extracts from Col or *spk1-1* plants, respectively; lanes 2, 5 and 3, 6 are coIP fractions using either α-SPK1N antibody or preimmune serum, respectively. The blot was probed with α-SPK1N (*Upper*) or α-NAP1 (*Lower*) antibody. (*C*) Endogenous SPK1 complexes are smaller when isolated in the *sra1* and *nap1* backgrounds. Crude extracts containing solubilized SPK1 were analyzed by size-exclusion chromatography. Column fractions were isolated from Col (*Top*), *sra1* (*Middle*), and *nap1* (*Bottom*). Apparent masses for column fractions are labeled. Vo, void volume. All fractions were probed with the α-SPK1N antibody.

full-length recombinant SPK1 and purified DHR2 with GDP–ROP, which is the physiologically relevant form of inactive ROP. Vertebrate DOCK family proteins such as Dock180 and Zizimin bind strongly only to nucleotide-depleted GTPase (18, 19, 22), and the ELMO proteins increase DOCK-mediated GEF activity (28). Our results suggest that SPK1 is sufficient for GEF activity, and based on the null phenotype of the *spk1-3* DHR2 truncation allele, the primary function of SPK1 may be to provide GEF activity. Interestingly, SPK1 binds to and activates ROPs promiscuously *in vitro*, suggesting that the biochemical selectivity of SPK1 for particular ROPs is not a major contributor to signaling specificity. The situation is quite different with vertebrate DOCKs. Nonplant DOCK GEFs display strong selectivity for Rac1 or Cdc42, and in these cases, the biochemical data correlate with *in vivo* signaling specificity (18, 19). It is possible that SRA1, the likely target of SPK1 signaling, contributes to ROP signaling specificity. Among the ROPs tested, SRA1 preferentially binds to ROP2 and ROP4, and this selectivity may limit the responsiveness of the WAVE complex to particular ROP signals. Clearly, further research is needed to determine whether particular ROPs function downstream of SPK1 and how signaling specificity is achieved.

In addition to generating ROP activation signals, SPK1 associates with downstream WAVE complex signaling targets. The binding of GEFs to their signaling effectors has been hypothesized as a general strategy to achieve specificity (3), and we provide strong support for such a regulatory scheme in the SPK1–WAVE–ARP2/3 pathway. In coIP experiments, we find that detergent-solubilized SPK1 complexes also contain the WAVE complex protein NAP1. It also is clear that the apparent mass of SPK1 complexes is reduced when isolated from *nap1* or *sra1* null plants. The recent report of yeast two-hybrid interactions between SPK1 and WAVE complex proteins is consistent with our results (29). It therefore is possible that SPK1 both generates and organizes ROP signaling. Interestingly, we find that overexpression of a constitutively active *ROP2* (CA-*ROP2*) (30) does not bypass the requirement for *SPK1*, because CA-*ROP2 spk1* plants have completely additive phenotypes when compared with the individual *spk1* and CA-*ROP2* lines. Perhaps additional ROPs are needed to activate the WAVE and ARP2/3 complexes. Alternatively, the subcellular location of ROP activation and/or the tight spatial coupling of ROP activation and its effector proteins are critical. Rac signaling can affect the composition (8) and the dynamic subcellular localization of WAVE complexes (9). SPK1 may define more precisely the location(s) of WAVE complex activation and/or the efficiency with which the WAVE complex proteins cycle through rounds of activation, use, and retrieval. Along these lines, it will be important to understand not only how ROP activation affects the association of WAVE complex proteins with SPK1 but also the downstream functions of WAVE and ARP2/3 during cell morphogenesis.

Although the results above firmly establish the existence of a SPK1–WAVE–ARP2/3 pathway, the components of this pathway are certain to have additional independent functions (SI Fig. 9). For example, the pavement cell and leaf shape defects of *spk1* are much more severe than those of *wave* and *arp2/3* mutants (5, 17, 31). Even in trichomes, *SPK1* is likely to have *WAVE–ARP2/3*-independent functions based on a reduced branch number phenotype that is not linked to an actin filament defect (24). Independent functions for *WAVE–ARP2/3* also are apparent because distorted trichome mutants have a cell-twisting phenotype that is not observed in *spk1* trichomes. Therefore, the *WAVE–ARP2/3* pathway controls coherent (nontwisting) cell elongation, and additional positive regulators of *SRA1* and the WAVE complex remain to be discovered (SI Fig. 9). We expect the shared and independent functions of *SPK1* and *WAVE–ARP2/3* to provide insight into how diverse cellular activities are integrated during morphogenesis.

In conclusion, this article demonstrates that the SPK1 DHR2 domain and its associated GEF activity generates ROP signals that positively regulate ARP2/3 and actin filament nucleation. SPK1 shares amino acid identity with DOCK family GEFs in several regions (17), and the fact that human and *Arabidopsis* WAVE complex proteins can function interchangeably (5, 27) suggests that the DOCK–WAVE–ARP2/3 pathway we describe here may be widely used in other multicellular organisms. Further study of SPK1 will continue to provide mechanistic knowledge about the architecture and regulation of evolutionarily conserved cell-shape control pathways.

Materials and Methods

Plant Strains, Growth Conditions, and Morphometry. For all experiments, the accession Col-0 was used as wild type. The *spk1-1* and *spk1-2* alleles are described in ref. 17. *spk1-3* is a TILLING allele (32) and was backcrossed four times before use. For all experiments, the null allele of *sra1* is *pir-3* (5). Cotyledon measurements and scanning electron microscopy (SEM) were conducted as described in ref. 17. For trichome morphometry, orthogonal views were used to measure the length, perimeter, and area. Swelling factor [$36 \times (\text{area})/\sqrt{3} \times (\text{perimeter})^2$)] is a dimensionless shape descriptor that we adapted to trichomes by using the equilateral triangle as the reference shape. The randomly positioned *sra1* trichome branches precluded its inclusion in the double mutant analysis.

coIP and Size-Exclusion Chromatography. To prepare plant extracts, 2 g of shoot tissue at 15 days after germination (DAG) was homogenized, solubilized, and clarified as described in *SI Methods*. For coIP, 700 μg of cell extracts were added to coIP buffer (20 mM Hepes/KOH, pH 7.2/150 mM NaCl/1% Nonidet P-40/0.1% SDS) containing 15 μg of α-SPK1N antibody or preimmune serum bound to protein A beads (Pierce). The protein A bound fractions were washed extensively and probed with α-SPK1N, α-NAP1, or α-ROP antibodies at dilutions of 1:1,000, 1:250, and 1:1,000, respectively. For size-exclusion chromatography, solubilized SPK1 fractions were separated on a Sephadex 200 HR 10/300 column (GE Healthcare). The column fractions were precipitated and analyzed by Western blotting using the α-SPK1N antibody. Gel-filtration experiments were repeated at least two times for each genotype.

Recombinant Protein Expression and Quantification. The construction of expression plasmids is described in *SI Methods*, and PCR primers used are described in SI Table 3. For expression and purification of the GST–996-DHR2 protein and HIS–SRA1, pDS15–996-DHR2 and pDS17–PIR(SRA1) plasmids were transformed into *Escherichia coli* Rosetta (DE3) strain (Novagen) and induced at OD_{600} = 0.6–0.7 and then grown at 37°C for 4 h. Soluble proteins were purified by using glutathione beads (Sigma-Aldrich) and Ni^{2+} beads (Novagen) according to the manufacturer's specifications. Full-length recombinant SPK1 was expressed by using the Bac-to-Bac SF9 insect cell expression system (Invitrogen). The concentration of SPK1 in the crude insect extracts was quantified by using a dot-blot assay with a purified SPK1 N-terminal protein fragment as a standard. The active fraction of recombinant full-length SPK1 and GST–996-DHR2 used in GEF assays was calculated based on the proportions of these proteins that bound to saturating amounts of nucleotide-depleted ROP2 in pull-down assays. See *SI Methods* for a description of the nucleotide-binding assay and GEF assay methodology.

Protein Pull-Down Experiments. For the GST–ROP pull-down assay using plant extracts, 3 μM bead-bound GST–ROP2 was mixed with 200 μg of soluble plant protein extract. The binding reactions were incubated at room temperature for 2 h. After extensive washing, the bead-bound fractions were probed with the α-SPK1N antibody. The GST–ROP pull-down assays with insect-expressed SPK1 used similar methods. For GST pull-down assays with GST–996-DHR2, 0.2 μM nucleotide-loaded HIS–ROP2 was incubated with bead-bound 0.05 μM GST–996-DHR2 for 2 h at room temperature, and the bead-bound fractions were probed with an α-ROP antibody.

ACKNOWLEDGMENTS. We thank Zhenbiao Yang (University of California, Riverside, CA) for the generous gift of the ROP2 and ROP10 expression clones and the CA-*ROP2*-expressing transgenic line, Johnathon Chernoff (Fox Chase Cancer Center, Philadelphia, PA) for the gift of the GST–Rac1 clone, and the *Arabidopsis* Biological Resource Center for DNA and seed stock distribution. We also thank Lacey Samuels for helpful comments on the manuscript. This work was supported by the Purdue Agricultural Research Program and National Science Foundation Molecular and Cellular Biosciences (MCB) Grant 0640872 (to D.B.S.).

1. Molendijk AJ, Ruperti B, Palme K (2004) Small GTPases in vesicle trafficking. *Curr Opin Plant Biol* 7:694–700.
2. Yang Z, Fu Y (2007) ROP/RAC GTPase signaling. *Curr Opin Plant Biol* 10:490–494.
3. Schmidt A, Hall A (2002) Guanine nucleotide exchange factors for Rho GTPases: Turning on the switch. *Genes Dev* 16:1587–1609.
4. Rossman KL, Channing JD, Sondek J (2005) GEF means go: Turning on RHO GTPases with guanine nucleotide-exchange factors. *Nat Rev Mol Cell Biol* 6:167–180.
5. Basu D, El-Assal SE, Le J, Mallery EL, Szymanski DB (2004) Interchangeable functions of Arabidopsis PIROGI and the human WAVE complex subunit SRA-1 during leaf epidermal development. *Development* 131:4345–4355.
6. Fu Y, Gu Y, Zheng Z, Wasteneys GO, Yang Z (2005) Arabidopsis interdigitating cell growth requires two antagonistic pathways with opposing action on cell morphogenesis. *Cell* 11:687–700.
7. Lavy M, *et al.* (2007) A novel ROP/RAC effector links cell polarity, root-meristem maintenance, and vesicle trafficking. *Curr Biol* 17:947–952.
8. Eden S, Rohatgi R, Podtelejnikov AV, Mann M, Kirschner MW (2002) Mechanism of regulation of WAVE1-induced actin nucleation by Rac1 and Nck. *Nature* 418:790–793.
9. Steffen A, *et al.* (2004) Sra-1 and Nap1 link Rac to actin assembly driving lamellipodia formation. *EMBO J* 23:749–759.
10. Szymanski DB (2005) Breaking the WAVE complex: The point of Arabidopsis trichomes. *Curr Opin Plant Biol* 8:103–112.
11. Basu D, *et al.* (2005) DISTORTED3/SCAR2 is a putative Arabidopsis WAVE complex subunit that activates the Arp2/3 complex and is required for epidermal morphogenesis. *Plant Cell* 17:502–524.
12. Nolan KM, *et al.* (1998) Myoblast city, the Drosophila homolog of DOCK180/CED-5, is required in a rac signaling pathway utilized for multiple developmental processes. *Genes Dev* 12:3337–3342.
13. Hudson AM, Cooley L (2002) A subset of dynamic actin rearrangements in Drosophila requires the Arp2/3 complex. *J Cell Biol* 156:677–687.
14. Berken A, Thomas C, Wittinghofer A (2005) A new family of RhoGEFs activates the Rop molecular switch in plants. *Nature* 436:1176–1180.
15. Gu Y, Li S, Lord EM, Yang Z (2006) Members of a novel class of Arabidopsis Rho guanine nucleotide exchange factors control Rho GTPase-dependent polar growth. *Plant Cell* 18:366–381.
16. Kaothien P, *et al.* (2005) Kinase partner protein interacts with the LePRK1 and LePRK2 receptor kinases and plays a role in polarized pollen tube growth. *Plant J* 42:492–503.
17. Qiu JL, Jilk R, Marks MD, Szymanski DB (2002) The Arabidopsis SPIKE1 gene is required for normal cell shape control and tissue development. *Plant Cell* 14:101–118.
18. Cote J-F, Vuori K (2002) Identification of an evolutionarily conserved superfamily of DOCK180-related proteins with guanine nucleotide exchange activity. *J Cell Sci* 115:4901–4913.
19. Meller N, Irani-Tehrani M, Kiosses WB, Del Pozo MA, Schwartz MA (2002) Zizimin1, a novel Cdc42 activator, reveals a new GEF domain for Rho proteins. *Nat Cell Biol* 4:639–647.
20. Vernoud V, Horton AC, Yang Z, Nielsen E (2003) Analysis of the small GTPase gene superfamily of Arabidopsis. *Plant Physiol* 131:1191–1208.
21. Lavy M, Bracha-Drori K, Sternberg H, Yalovsky S (2002) A cell-specific, prenylation-independent mechanism regulates targeting of type II RACs. *Plant Cell* 14:2431–2450.
22. Brugnera E, *et al.* (2002) Unconventional Rac-GEF activity is mediated through the Dock180-ELMO complex. *Nat Cell Biol* 4:574–582.
23. Mathur J, Spielhofer P, Kost B, Chua N (1999) The actin cytoskeleton is required to elaborate and maintain spatial patterning during trichome cell morphogenesis in Arabidopsis thaliana. *Development* 126:5559–5568.
24. Szymanski DB, Marks MD, Wick SM (1999) Organized F-actin is essential for normal trichome morphogenesis in Arabidopsis. *Plant Cell* 11:2331–2347.
25. Li Y, Sorefan K, Hemmann G, Bevan MW (2004) Arabidopsis *NAP* and *PIR* regulate actin-based cell morphogenesis and multiple developmental processes. *Plant Physiol* 136:3616–3627.
26. Manser E, *et al.* (1998) PAK kinases are directly coupled to the PIX family of nucleotide exchange factors. *Mol Cell* 1:183–192.
27. El-Assal SE, Le J, Basu D, Mallery EL, Szymanski DB (2004) Arabidopsis GNARLED encodes a NAP125 homologue that positively regulates ARP2/3. *Curr Biol* 14:1405–1409.
28. Lu M, *et al.* (2004) PH domain of ELMO functions in trans to regulate Rac activation via DOCK180. *Nat Struct Mol Biol* 11:756–762.
29. Uhrig JF, *et al.* (2007) The role of Arabidopsis SCAR genes in ARP2-ARP3-dependent cell morphogenesis. *Development* 134:967–977.
30. Fu Y, Li H, Yang Z (2002) The ROP2 GTPase controls the formation of cortical fine F-actin and the early phase of directional cell expansion during Arabidopsis organogenesis. *Plant Cell* 14:777–794.
31. Le J, El-Assal SE, Basu D, Saad ME, Szymanski DB (2003) Requirements for Arabidopsis ATARP2 and ATARP3 during epidermal development. *Curr Biol* 13:1341–1347.
32. McCallum CM, Comai L, Greene EA, Henikoff S (2000) Targeting induced local lesions IN genomes (TILLING) for plant functional genomics. *Plant Physiol* 123:439–442.